Dynamics of Atomic and Molecular Hydrogen Elimination from Small Alkanes Following 157-nm Excitation

S. M. Wu,[†] J. J. Lin,[‡] Y. T. Lee,[†,‡] and X. Yang*[,‡,§]

Department of Chemistry, National Taiwan University, Taipei, Taiwan, Institute of Atomic and Molecular Sciences, Academia Sinica, Taipei, Taiwan, and Department of Chemistry, National Tsing Hua University, Hsinchu, Taiwan

Received: February 2, 2000; In Final Form: May 3, 2000

Photodissociation of a series of C_3-C_9 alkanes following 157 nm excitation has been investigated using the photofragment translational spectroscopy (PTS) technique. Three series of alkanes, normal alkanes, branched alkanes, and cyclic alkanes, were studied and the atomic hydrogen (H) and molecular hydrogen (H_2) elimination from their photodissociation were experimentally investigated. Experimental results show that the dynamics of the H and H_2 elimination processes from larger *n*-alkanes is quite similar to that of propane. Dissociation of the branched alkanes is, however, significantly different from that of the normal alkanes. C−C bond fission is more significant in the branched alkanes. There are also notable differences among the branched alkanes for the H and H_2 elimination processes. Photodissociation dynamics of small cyclic alkanes are significantly different from that of the acyclic alkanes. This is likely due to their significantly different electronic structures caused by the large ring strain in small cyclic alkanes. The H and H_2 elimination channels for larger cyclic alkanes are quite similar to the normal alkanes. Relative branching ratios of the H and H_2 elimination channels for all the alkane molecules are determined and compared.

I. Introduction

Small alkanes, such as methane, ethane, and propane, are the main constituents in the natural gas that is widely used in heating and cooking. The combustion processes in mechanical engines and burning flames all involve dissociation of the alkane molecules at high temperature. Even though dissociation of the alkane molecules is pervasive in combustion and pyrolysis processes, the fundamental dissociation dynamics of these dissociation processes are not well understood at the molecular level. The dissociation dynamics of alkanes have rarely been experimentally studied using modern experimental techniques. This is partly due to the lack of a strong photolysis laser source in the vacuum ultraviolet (VUV) region, in which most alkanes start to absorb, or suitable infrared (IR) multiphoton sources. IR multiphoton dissociation of alkanes can most closely mimic the pyrolysis process because IR multiphoton pumping is very similar to the normal heating process. Photodissociation studies in the VUV region can also provide useful information on the dissociation dynamics of these important molecules.

Dynamics of the atomic hydrogen elimination processes from the photodissociation of CH_4 at Lyman-α (121.6 nm) have been extensively investigated in detail with its isotopomers in recent few years.[1−5] Two distinctive binary dissociation processes of H-atom elimination and one triple-dissociation channel have been observed by Liu and co-worker.[4] Several possible dissociation channels of the photodissociation of CH_4 have been theoretically predicted by Mebel et al.[6] The fast binary dissociation channel ($CH_3 + H$) involves a parallel-type excitation followed by internal conversion to the ground-state surface on which dissociation occurs. The other one involves a perpendicular-type excitation followed by intersystem crossing to the triplet

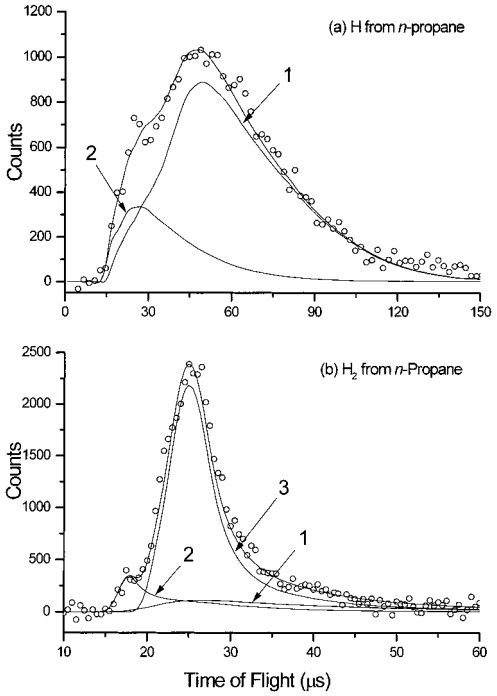

Figure 1. TOF spectra of the photodissociation products (H and H_2) from *n*-propane at 157 nm. (a) H products from *n*-propane; curve 1 is the contribution of H atoms from the internal carbon site, while curve 2 represents H-atom products from the terminal carbon site. (b) H_2 products from *n*-propane; curve 1 represents contribution of 1,1-H_2 three-center elimination from terminal CH_3 groups, curve 2 is the contribution of 1,2-H_2 four-center elimination, and curve 3, is due to the 2,2-H_2 three-center elimination from the middle CH_2 group. For a more detailed description of these results, please see refs 15 and 16.

* To whom correspondence should be addressed. E-mail: xmyang@po.iams.sinica.edu.tw.
[†] National Taiwan University.
[‡] Academia Sinica.
[§] National Tsing Hua University.

10.1021/jp0004056 CCC: $19.00
Published on Web 07/13/2000

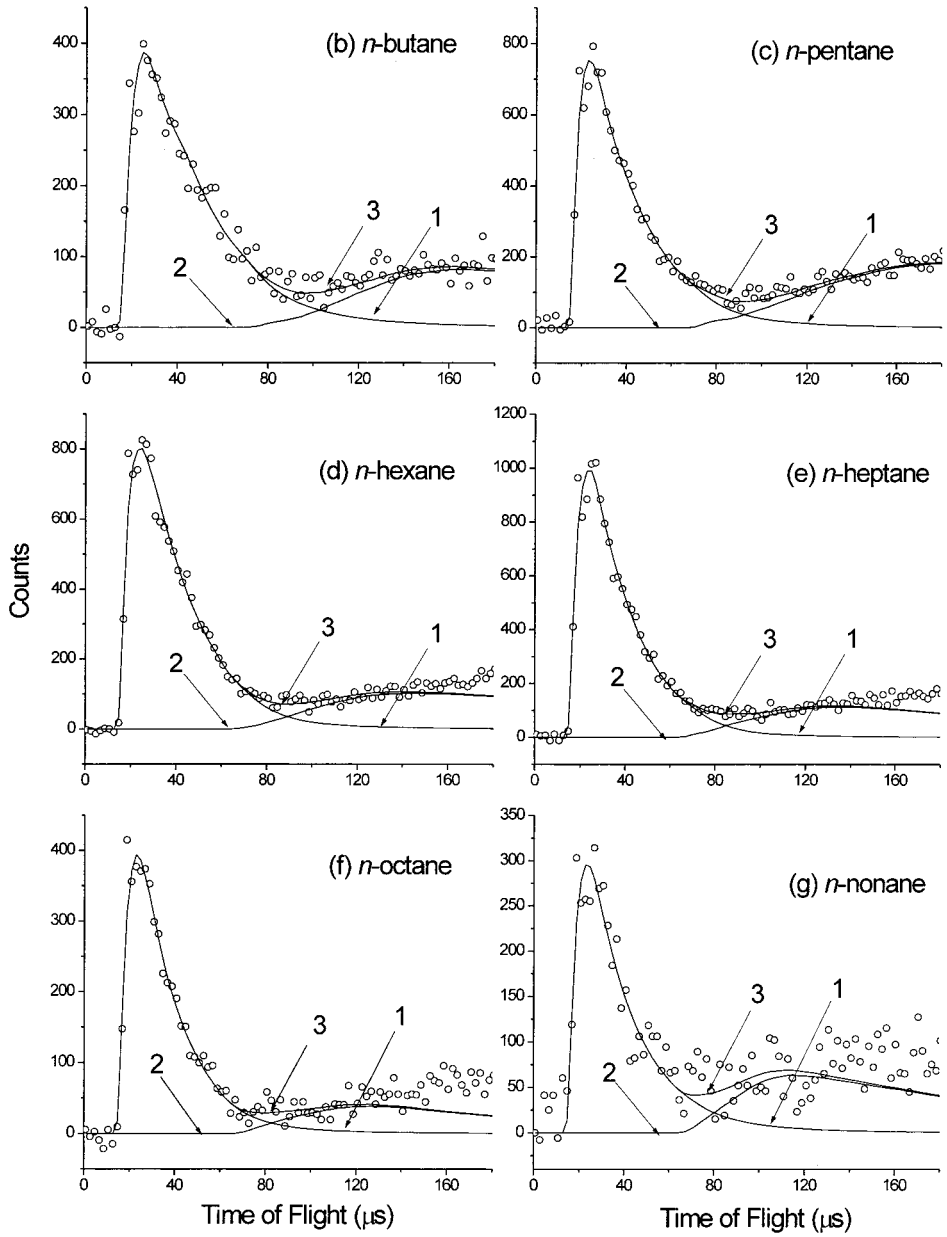

Figure 2. TOF spectra at mass 1 from some normal alkanes at 157 nm. The open circles are the experimental data points, while the solid curves are the fits to the spectra using the translational energy distributions of H elimination as shown in Figure 4. For all spectra, curve 1 is the contribution from the H-atom products, curve 2 is the contribution from the cracking of CH_3 products, and curve 3 is the overall fit.

surface and then dissociation. The theoretical investigations have also supported the experimental results. The site specificity of the atomic elimination process from the photodissociation of propane at 157-nm excitation has been investigated using the Doppler spectroscopic technique by Tonokura et al.[7] Their experimental results showed that the atomic hydrogen products mostly come from the terminal carbons of propane. CH_3CH_3 and $CH_3CH_2CH_3$ at Lyman-α excitation (121.6 nm) have been recently studied using the velocity map imaging technique.[8] Two types of H elimination are identified, one formed along with an alkyl radical in a Rydberg state and other by its subsequent decomposition. It has also been established that molecular detachment processes play a major role in the photolysis of ethane (CH_3CH_3),[9] propane ($CH_3CH_2CH_3$),[10,11] and *n*-butane ($CH_3CH_2CH_2CH_3$)[11−13] under VUV light excitation, though it is a minor process in the photodissociation of methane (CH_4),[3,14] Chandler and co-workers have also measured the $H_2(v,J)$ photofragment images following the two-photon absorption that deposits 10.8−11.8 eV of energy in the methane molecule.[3] They observed that there are two molecular hydrogen elimination channels: the direct two-body dissociation process ($CH_4 \rightarrow CH_2 + H_2$) and the triple-dissociation process ($CH_4 \rightarrow CH + H_2 + H$). Very recently, we have also studied the photodissociation of propane and other hydrocarbon molecules at 157 nm, where site-specific phenomena for both atomic and molecular hydrogen elimination processes have been clearly observed.[15,16]

The absorption spectra of the alkanes from propane to *n*-octane in the VUV region are continuous with no clear vibrational structure.[17−22] There is a weak absorption shoulder between 163.0 and 157.5 nm in all the spectra from ethane to *n*-octane. However, no clear consensus has been reached yet on the assignment of these transitions. Raymonda and Simpson assigned them to an intramolecular charge-transfer excitation between adjacent C−C bonds,[23] while Robin assigned them to a Rydberg excitation to 3s,[24] and Sandorfy and co-workers suggested the excitation is localized mainly in one ethyl group.[17] Theoretical calculations[25,26] show that the vertical transition

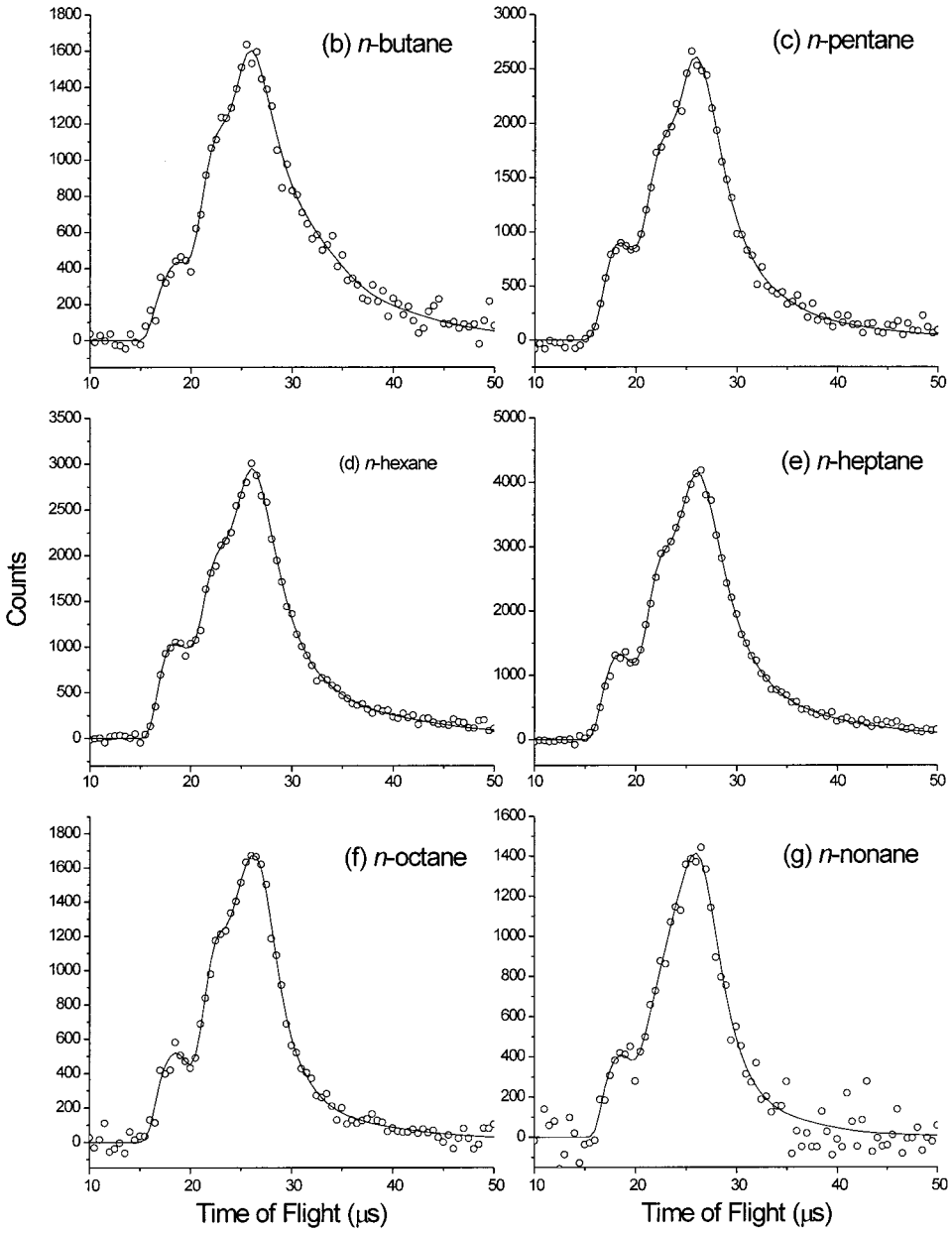

Figure 3. TOF spectra at mass 2 from some normal alkanes at 157 nm. The open circles are the experimental data points, while the solid curves are the fits to the spectra using the translational energy distributions of H_2 elimination as shown in Figure 5.

energy to the 3s Rydberg orbital is about 1 eV higher than the starting absorption energy of the first absorption shoulder. This, however, is not necessarily contradictory to the assignment of the lowest absorption of propane to the 3s Rydberg absorption because the vertical transition energy could be much higher than the adiabatic transition energy as a result of large geometric changes between the initial and final electronic states.[6] More extensive theoretical investigations are required to assign these transitions clearly.

The present work provides a systematic study on the photodissociation of alkanes for the atomic hydrogen and molecular hydrogen elimination processes using the photofragment translational spectroscopic technique. By measurement the product kinetic energy distributions, detailed dynamical information are obtained for the photodissociation processes of different alkane molecules.

II. Experimental Section

The photodissociation dynamics of small alkanes at 157 nm were investigated using the photofragment translational spectroscopic method. The experiments in this work were conducted using a crossed beam apparatus, which consists of two source chambers, a main chamber and a rotatable universal detector.[27] In a typical experiment, a molecular beam of alkane was crossed with a 157-nm laser beam perpendicularly, and photodissociation products were then detected by the universal time-of-flight (TOF) detector. The most crucial component for the apparatus used in this study is the extremely clean detector. Ultrahigh vacuum (1×10^{-12} Torr) is maintained in the electron-impact ionization region during the period of an experiment to make the detection of the molecular and atomic hydrogen products much easier than other similar apparatus.

In the normal alkane series, primary photodissociation at 157-nm excitation is not possible for methane (CH_4) and ethane (CH_3CH_3) because there is no absorption at this wavelength for CH_4 and only very weak absorption for CH_3CH_3, most probably because of hot band transitions. However, the photochemistry of propane or larger alkanes (up to *n*-nonane) at 157 nm could be investigated because these molecules have both

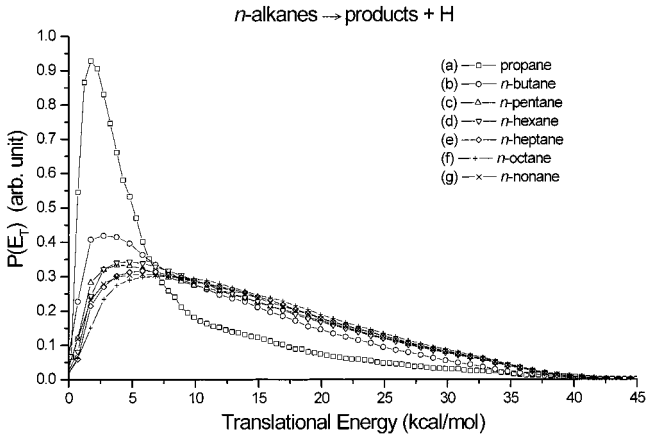

Figure 4. Translational energy distributions for atomic hydrogen (H) elimination from photodissociation of some normal alkanes at 157 nm. The relative heights of the distributions are arbitrary.

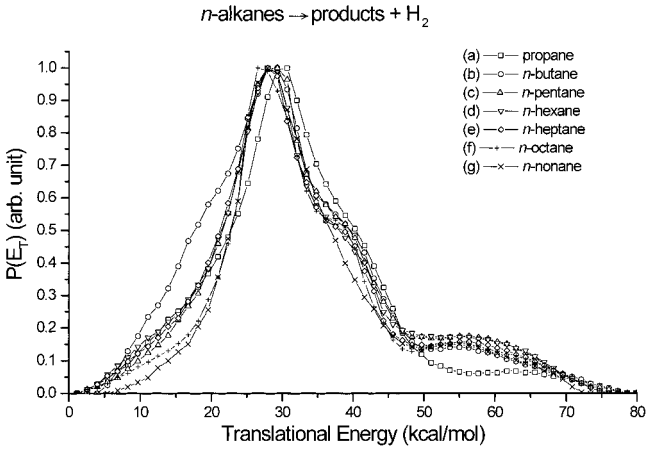

Figure 5. Translational energy distributions for molecular hydrogen (H_2) elimination from the photodissociation of some normal alkanes at 157 nm. The relative heights of the distributions are arbitrary.

significant absorption cross sections as well as substantial vapor pressures at room temperature. In the branched alkane series, the butane isomer (isobutane), pentane isomers (2-methylbutane), and hexane isomers (2-methylpentane, 3-methylpentane, 2,2-dimethylbutane, and 2,3-dimethylbutane) were studied. In the cyclic alkane series, the photochemistry of the series cyclopropane (C_3H_6) to cyclooctane (C_8H_{16}) was investigated. (Cyclobutane was not commercially available; therefore, it was not studied experimentally.) All the alkane samples were obtained commercially and used without further purification.

The light source used in this study was an unpolarized 157-nm laser beam generated by a Lambda Physik LPX 210*i* F_2 laser with a NOVA tube laser cavity. The repetition rate used in the experiment was 50 Hz and the laser pulse duration was about 15 ns. A differentially pumped laser beam path was used, and the vacuum of the laser beam path was $\sim 1 \times 10^{-7}$ Torr or better. About 1 mJ/pulse laser light was loosely focused into the interaction region, and the laser beam was normally attenuated by a mesh to minimize the multiphoton effect. The laser spot size is $\sim 4 \times 4$ mm in the interaction region. A 50-Hz-pulsed alkane molecular beam was produced by expanding the neat alkane samples from a solenoid valve (General Valve) through a 0.5-mm-diameter orifice. The backing pressure of the alkane samples during the experiment was typically 50 Torr, or lower if the vapor pressure at room temperature was <50 Torr.

Normally, the lighter photodissociation products (H and H_2) fly very fast so that the residence time of these photoproducts in the ionizer is quite short; therefore, the ionization efficiency for these products is small, typically $\sim 10^{-5}$. To compensate for this, the laser beam crossed the alkane molecular beam perpendicularly very close to the nozzle tip, at a distance of $\sim$5 mm away. The photodissociation products passed through a hole of 4-mm diameter on the cold plate near the source chamber wall and then entered the detector through a square hole on the front wall of the detector. The flight distance (L) of the neutral products was 285 mm and the detection axis was orthogonal to both the laser beam and the molecular beam. The neutral products were ionized by a Brink-type ionizer,[27] and the length of the ionization region (ΔL) was $\sim$13 mm. The ions were focused by some ion optics, then mass-selected by a quadrupole mass filter (Extrel), and finally counted by a Daly-type ion detector.[27] In this study, the data were accumulated over $(2 \times 10^4)-(4 \times 10^5)$ laser shots, depending on the S/N ratios. All experimental conditions such as molecular number density and laser intensity in the interaction region were well controlled to make meaningful comparisons. Multiphoton effects and molecular clustering effects were carefully checked.

TABLE 1: Relative Yields of Atomic Hydrogen (H) and Molecular Hydrogen (H_2) Elimination Channels from the Photodissociation of Some normal Alkanes

molecule	*n*-alkanes → products+H	*n*-alkanes → products+H_2
propane	1	2.1
n-butane	1	5.1
n-pentane	1	4.5
n-hexane	1	4.8
n-heptane	1	5.7
n-octane	1	5.6
n-nonane	1	7.3

Product TOF spectra from photodissociation of the alkane molecules were measured in the laboratory frame. To obtain the center-of-mass (CM) product translational energy distributions $P(E_T)$, conversions from the laboratory frame to the center-of-mass frame are required. Such conversions in this work were carried out using a forward convolution method with a recently developed software package, CMLAB3,[28] which was modified from the previous version, CMLAB2.[29] In this program, a trial $P(E_T)$, and a CM product angular distribution (β parameter) are used to calculate the TOF spectrum for the mass (m/e) of the photofragment at the angle (Θ_{lab}) between the molecular beam and the detector using the known apparatus parameters and the measured beam velocity distribution (v_{beam}). The calculated TOF spectrum was then compared with the experimental TOF spectrum and the $P(E_T)$ was adjusted point by point on a computer screen until a satisfactory fit was achieved for the TOF spectrum. All translational energy distributions were obtained assuming that the photodissociation products were from the binary dissociation processes. The relative branching ratios of the dissociation channels were also calculated by integrating the signals in the center-of-mass frame. In this work, the 157-nm photolysis laser source is unpolarized; therefore, the anisotropic effect on the branching ratios should be very small. In the data analysis in this work, this small effect is neglected.

III. Results and Discussions

TOF spectra of the products from the photodissociation of the alkane molecules at 157 nm were measured. Signals of the photodissociation of alkanes at $m/e = 1$, 2, 12, 13, 14, 15, and 16. After detailed analyses of the experimental data, H and H_2 elimination channels were identified for the photodissociation of all alkanes. All the translational energy distributions were

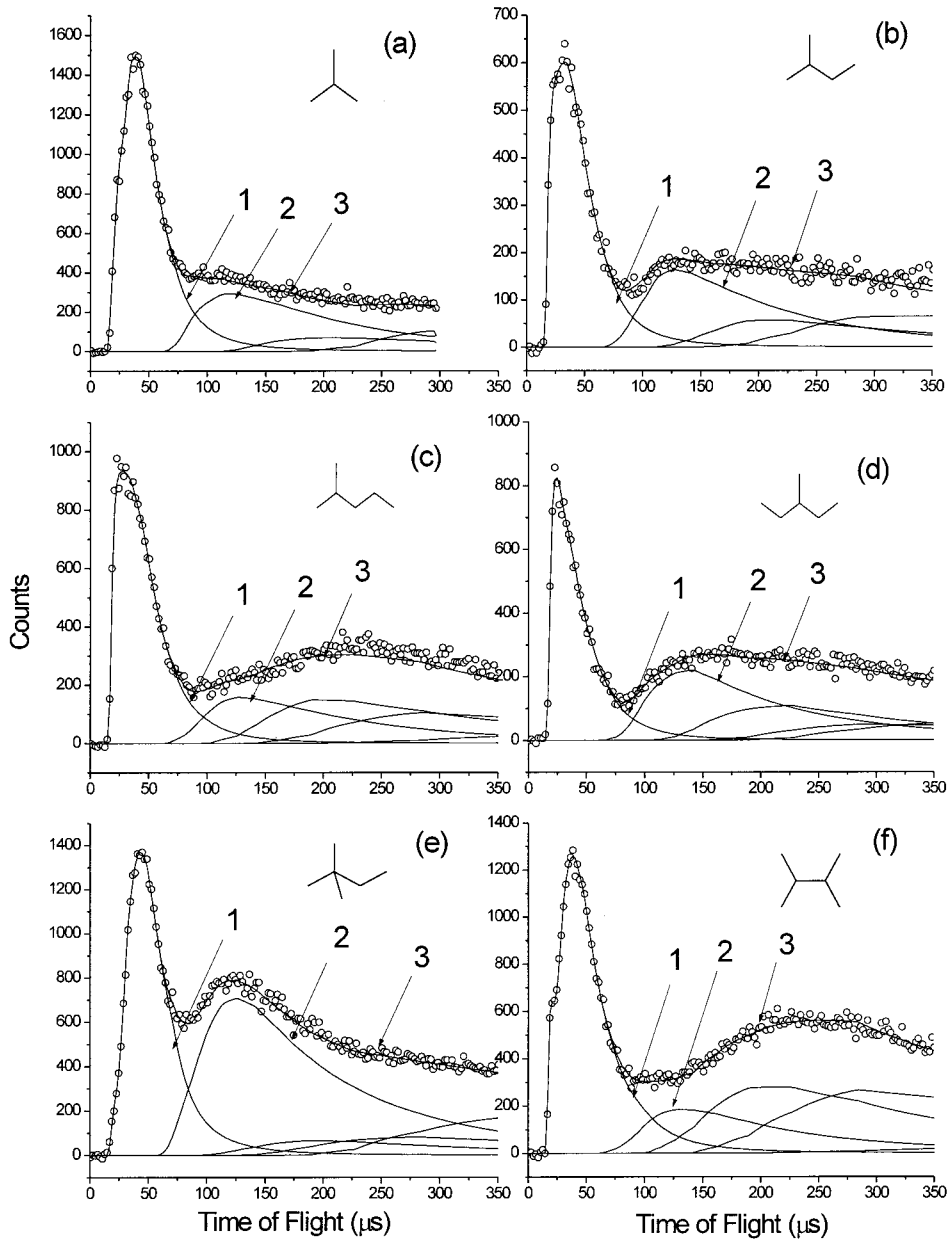

Figure 6. TOF spectra at mass 1 from some branched alkanes at 157 nm. The open circles are the experimental data points, while the solid curves are the fits to the spectra using the translational energy distributions of H elimination as shown in Figure 8. For all the spectra, curve1 is the contribution from the neutral H-atom product and curve 2 is the contribution from the cracking of CH_3 products (CH_3 elimination). The other slower curves are the contribution from the cracking of C_2H_5, C_3H_7 (other C−C bond cleavage processes), etc., by assuming the translational energy distributions the same as those of CH_3 elimination, and curve 3 is the overall fit. (a) *i*-butane, (b) *i*-pentane, (c) *i*-hexane, (d) 3-methylpentane, (e) *neo*-hexane, and (f) diisopropyl.

obtained assuming that that the dissociation products were from the binary dissociation processes. In this section, the experimental data and the detailed analyses for the photodissociation of the alkane molecules are described.

a. Photodissociation of Some Normal Alkanes. Photodissociation of *n*-butane, *n*-pentane, *n*-hexane, *n*-heptane, *n*-octane, and *n*-nonane were investigated in this study. To understand the dissociation dynamics of the normal alkanes, the results are compared with those of *n*-propane, studied previously in our laboratory.[15,16] Site specificity of the H and H_2 elimination processes from propane has been observed. The study of the site specificity of the H and H_2 elimination involves the photodissociation of the deuterium-labeled propane compounds ($CH_3CD_2CH_3$ and $CD_3CH_2CD_3$). Figure 1 shows the TOF spectra of the H and H_2 products from *n*-propane at 157 nm. For H-atom elimination, most H-atom products are from the terminal CH_3 group, which were attributed to secondary H-atom elimination following the primary H_2 elimination from the CH_2 group. In addition, there is also some contribution of primary H-atom elimination from the middle CH_2 group. For the H_2 elimination, most H_2 products are from the middle CH_2 group (2,2-H_2 elimination), while there are some contributions from the 1,1-H_2 elimination and the 1,2-H_2 elimination. TOF spectra of the photoproducts from the higher *n*-alkanes at $m/e = 1$ (H) and 2 (H_2) have been measured, and all TOF spectra obtained here were accumulated over 40−200-k laser shots depending on the signal levels.

TOF spectra at $m/e = 1$ from photodissociation of the *n*-alkanes are shown in Figure 2. Because dissociative ionization of a hydrogen molecule by electron bombardment at an electron energy of ~60 eV is negligible,[30] the H_2 contribution to the TOF spectrum at $m/e = 1$ can be neglected. The slower part

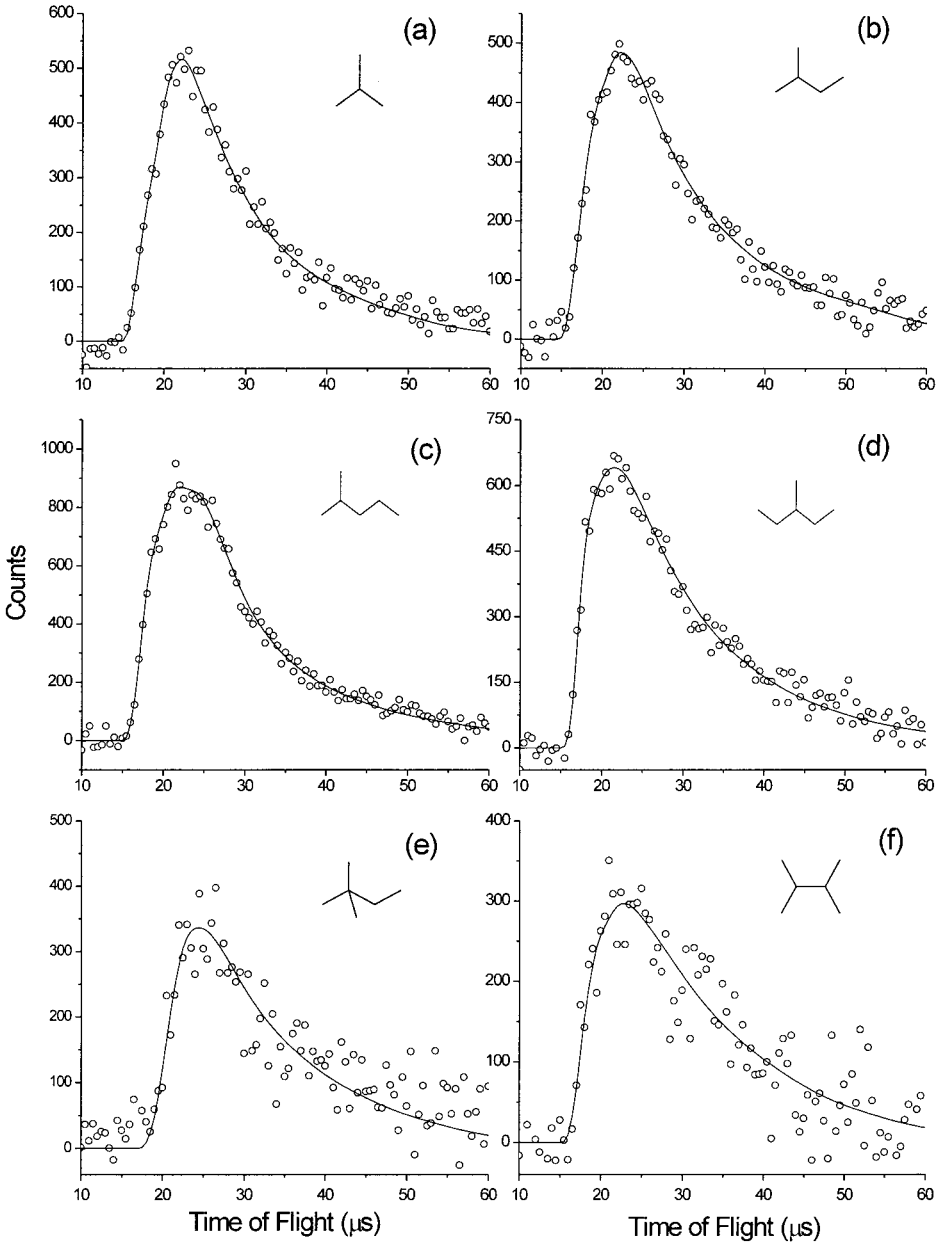

Figure 7. TOF spectra at mass 2 from some branched alkanes at 157 nm. The open circles are the experimental data points, while the solid curves are the fits to the spectra using the translational energy distributions of H_2 elimination as shown in Figure 9. (a) *i*-butane, (b) *i*-pentane, (c) *i*-hexane, (d) 3-methylpentane, (e) *neo*-hexane, and (f) diisopropyl.

(curve 2) of the TOF spectrum at $m/e = 1$ comes from the dissociative ionization of the CH_3 (CH_3 elimination) products from the C−C bond fission process, indicating that C−C bond rupture is quite significant in the *n*-alkane photodissociation. The fast peaks clearly come from the neutral H-atom products. These fast peaks were fitted as a binary H-atom elimination process using the translational energy distributions as shown in Figure 4. Similar to the propane H-atom elimination, the kinetic distributions for H-atom elimination can be divided into two contributions: lower and higher energy contributions. From our recent study on the propane photodissociation,[15,16] it is known that the lower energy contribution should come from secondary H-atom elimination from the two terminal CH_3 groups following the H_2 elimination from the middle CH_2 group while the higher energy contribution should be primary H-atom elimination from the middle CH_2 group. Assuming that the dynamics do not change significantly for these processes in higher *n*-alkanes, it is interesting to note that the lower energy contribution becomes much less significant in the photodissociation of higher *n*-alkanes relative to the higher energy contribution. For the higher alkanes, the kinetic energy distributions for the H-atom elimination process are almost identical to rather high kinetic energy release. These results imply that the dominant H-atom elimination process for a larger alkane molecule should be the H-atom elimination from the CH_2 groups rather than from the terminal CH_3 groups. This is quite reasonable because higher *n*-alkanes have more internal H atoms. It is difficult, though, to determine the relative yields of various H-atom elimination processes from different sites in these alkanes quantitatively.

TOF spectra of photodissociation products at mass 2 from the *n*-alkanes are shown in Figure 3. These TOF spectra were simulated using the translational energy distributions for the binary molecular hydrogen elimination processes as shown in Figure 5. From our previous investigation of the H_2 elimination from propane,[15,16] it was clear that the faster peak at ∼60 kcal/

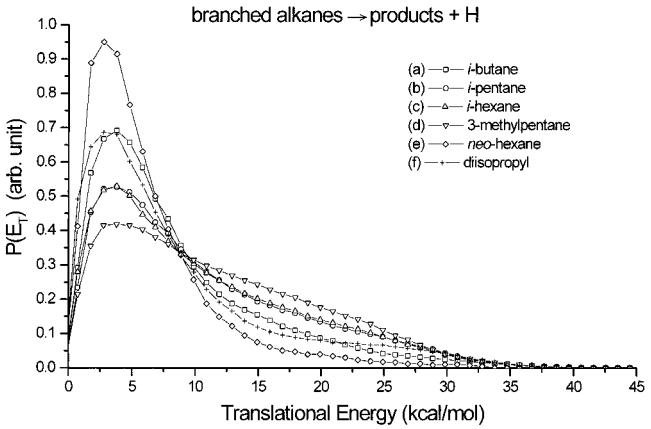

Figure 8. Translational energy distributions for atomic hydrogen (H) elimination from the photodissociation of some branched alkanes at 157 nm. The relative heights of the distributions are arbitrary.

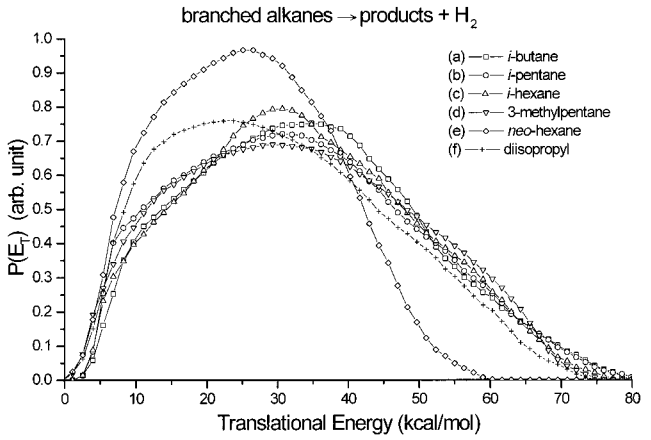

Figure 9. Translational energy distributions for molecular hydrogen (H_2) elimination from the photodissociation of some branched alkanes at 157 nm. The relative heights of the distributions are arbitrary.

mol in the kinetic energy distribution for propane (Figure 5) is from the four-center H_2 elimination, while the main slower peak at ~30 kcal/mol is from the three-center H_2 elimination from the middle CH_2 group. As we can see from Figure 5, the translational energy distributions for H_2 elimination for larger *n*-alkanes are very similar to each other. They are also similar to that of propane. There are, however, some noticeable differences in the translational energy distributions of these molecules. For example, the higher energy component at about 60 kcal/mol for higher alkanes is more pronounced than that of propane, implying that the four-center H_2 elimination is more important for larger alkanes. There are also some differences near the shoulder around 40 kcal/mol, which should come from the H_2 elimination from the CH_2 groups. In addition, the lower energy part of the distribution for butane is notably higher than others. Despite all these differences, the overall pictures for different *n*-alkanes are remarkably similar to each other, indicating the similar nature of the dynamics of the H_2 elimination processes from these molecules. This is likely due to the similar electronic structures of excited electronic states for these normal alkanes. The above experimental results also indicate that the three-center internal-H_2 elimination and four-center H_2 elimination processes are dominant processes in all alkanes, but the quantitative information on the site specificity of the H_2 elimination for each individual alkane molecule still needs further isotopic labeling studies.

The relative branching ratios for the H and H_2 elimination channels have been determined and the results are listed in Table 1. All the relative yields have been calibrated by the detection efficiencies of the H and H_2 products. The importance of the H_2 elimination from *n*-butane to *n*-octane is generally increasing relative to the H-atom elimination. This is quite reasonable because the dominant process of H_2 elimination from alkane seems to be from the H_2 elimination from the central carbon atoms. The increase of the H_2 elimination is at least partly due to the increasing number of the CH_2 groups in larger alkane molecules. From the above results, it is clear that slow H-atom elimination from the terminal CH_3 groups is significantly reduced for that from larger *n*-alkanes. This would also reduce the branching of the H-atom elimination for larger alkanes and thus enhance the branching of the H_2 elimination process.

TABLE 2: Relative Yields of Atomic Hydrogen (H) and Molecular Hydrogen (H_2) Elimination Channels from the Photodissociation of Some Branched Alkanes

molecule	branched alkanes → products+H	branched alkanes → products+H_2
i-butane	1	0.59
i-pentane	1	1.4
i-hexane	1	2.0
3-methylpentane	1	2.1
neo-hexane	1	0.18
diisopropyl	1	0.26

b. Photodissociation of Some Branched Alkanes. Photodissociation of 2-methylpropane (*i*-butane), 2-methylbutane (*i*-pentane), 2-methylpentane (*i*-hexane), 3-methylpentane, 2,2-dimethylbutane (*neo*-hexane), and 2,3-dimethylbutane (diisopropyl) following 157-nm excitation was also investigated in this work. TOF spectra of the photodissociation products from these branched alkanes at $m/e = 1$ (H) and 2 (H_2) were measured. These TOF spectra were accumulated over 20−50-k laser shots.

Figure 6 shows the TOF spectra at $m/e = 1$ from the branched alkanes. The contribution described by curve 2 in these TOF spectra comes from the dissociative ionization of the CH_3 (CH_3 elimination) products, which were detected at mass 15. The even slower parts were attributed to heavier photofragments such as ethyl, propyl, and butyl radicals from the C−C bond fission process and were fitted by assuming that the translational energy distributions for these C−C bond rupture processes are the same. It is quite obvious that contributions of the cracking of heavier fragments to the $m/e = 1$ signal are larger than those observed in *n*-alkanes, indicating that C−C bond fission should be more important than the normal alkanes. In fact, C−C bond fission is likely the most important process in the photodissociation of branched alkanes at 157 nm. It is difficult, however, to estimate relative branching ratios of these processes. The fast peak in these TOF spectra should all come from the H-atom products (curve 1) and was fitted as a binary atomic hydrogen elimination process. The translational energy distributions for the H-atom elimination from the branched alkanes are presented in Figure 8. It is interesting to note that the distributions for *i*-butane (curve a) and diisopropyl (curve f) are very similar, while the distributions for *i*-pentane (curve b) and *i*-hexane (curve c) are also very similar to each other. There are only primary and tertiary hydrogen atoms for *i*-butane and diisopropyl, and similarly primary, secondary, and tertiary hydrogen atoms for *i*-pentane and *i*-hexane. This implies that the dynamics of the H elimination likely depend on the geometric complexities of the alkanes. As we can see in Figure 7, the slower part for *neo*-hexane is the largest among this group of molecules, while that for 3-methylpentane is the smallest. This indicates that more methyl groups near the higher order carbon atoms (4° and 3°) should produce more secondary H photodissociation products,

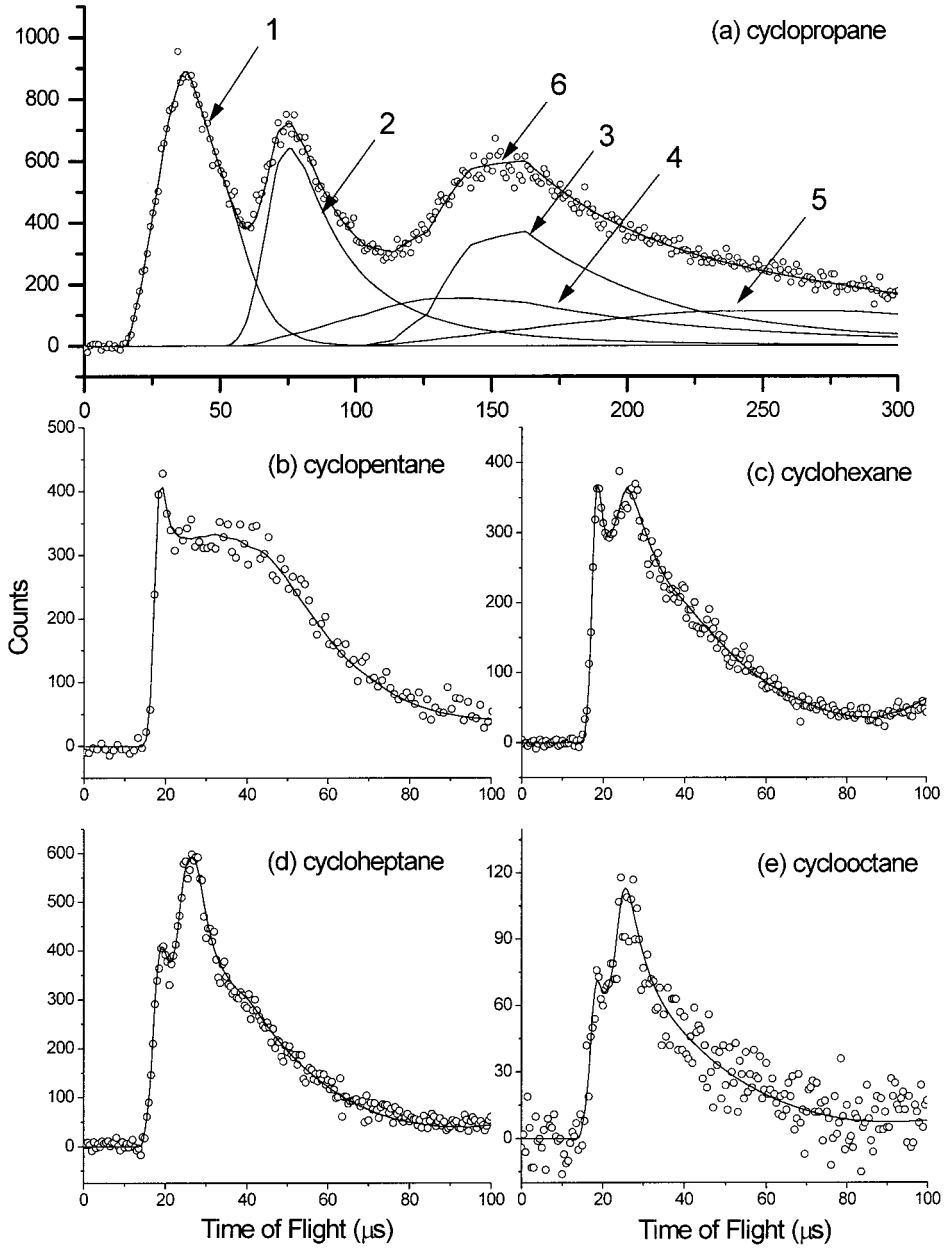

Figure 10. TOF spectra at mass 1 from some cyclic alkanes at 157 nm. The open circles are the experimental data points, while the solid curves are the fits to the spectra using the translational energy distributions of H elimination as shown in Figure 12. For the TOF spectra of (a) cyclopropane, curve 1 is the contribution from the H products; curve 2 is the contribution from the cracking of CH_2 products and curve 3 is from the momentum-matched contribution of the photodissociation partner, C_2H_4; curve 4 is from the cracking of CH_3 products and curve 5 is from the momentum-matched contribution of the photodissociation partner, C_2H_3; curve 6 is the overall fit.

similar to the propane photodissociation. This also implies that the more branched the alkane, the slower the H-atom products.

TOF spectra at mass 2 from photodissociation of the branched alkanes at $m/e = 2$ are shown in Figure 7. Because dissociative ionization of the higher mass radical products normally does not produce $m/e = 2$ signals in the electron bombardment ionizer, all signals observed at $m/e = 2$ should come from the H_2 photodissociation products. These TOF spectra were simulated using the translational energy distributions as shown in Figure 9. It is apparent that the distributions of the H_2 elimination process for the branched alkanes are significantly different from those of the normal alkanes, indicating the dynamics of the H_2 elimination for these two series of molecules are quite different from each other. This is not surprising because the electronic structures of the branched alkanes should be notably different from those of the normal alkanes. The translational energy distributions for the H_2 elimination of the branched alkanes are significantly broader than those of the normal alkanes, indicating that the H_2 elimination process for branched alkanes at 157-nm excitation are likely more statistical than that of the normal alkanes, which are quite dynamical. The distributions for *i*-butane (curve a), *i*-pentane (curve b), *i*-hexane (curve c), and 3-methylpentane (curve d) are very simliar, while the distributions for diisopropyl (curve f) and *neo*-hexane (curve e) are significantly different from the other compounds.

The relative branching ratios for the H and H_2 elimination channels have also been determined and the results are listed in Table 2. All relative yields have been calibrated by the detection efficiencies of the H and H_2 products. From Table 2, the more branched alkanes produce more atomic hydrogen products than molecular hydrogen products. The H_2/H branching ratios for 2-methylpentane (*i*-hexane) and 3-methylpentane are nearly the same; this is likely due to the fact that the two isomers are similar except that the methyl group is substituted at carbon

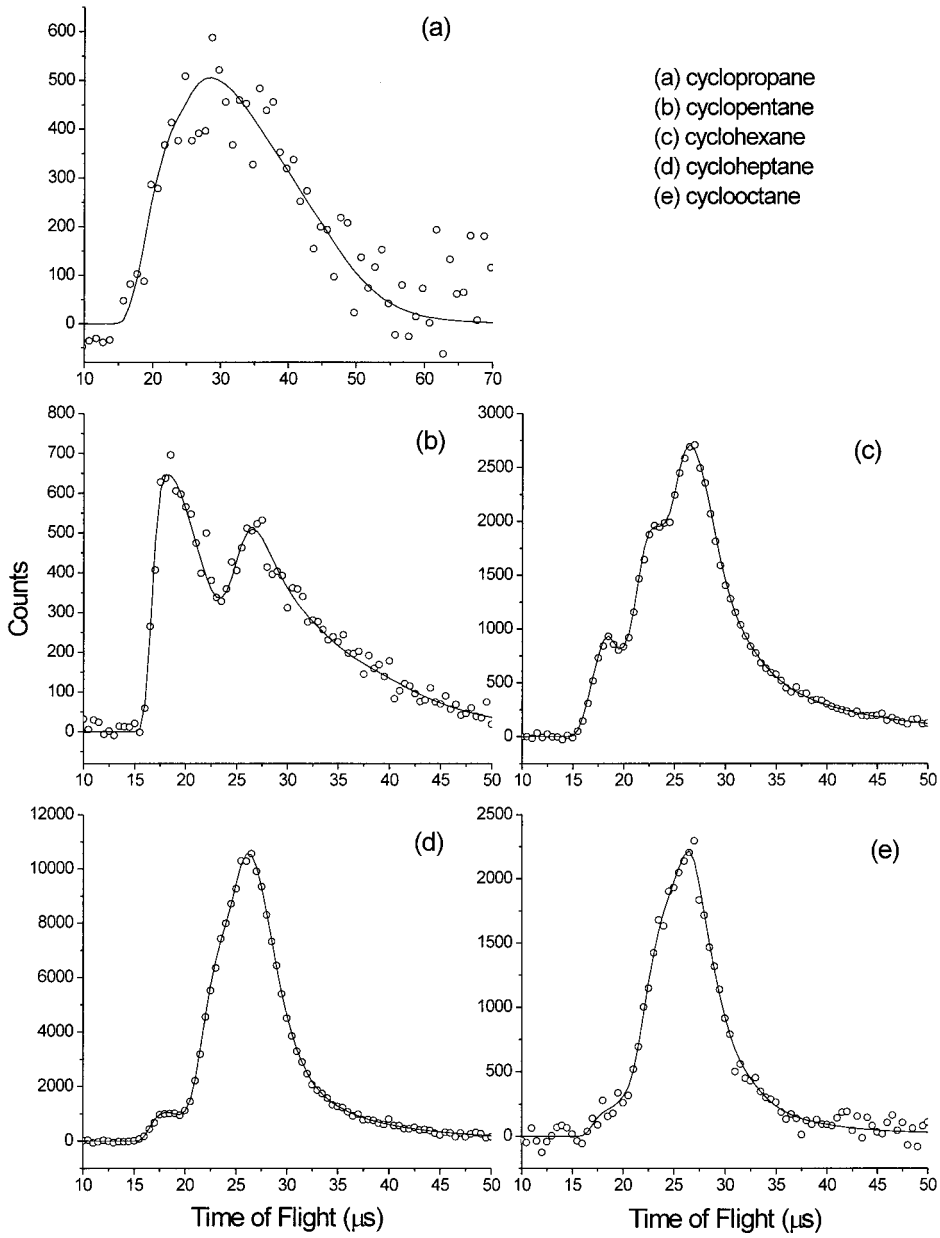

Figure 11. TOF spectra at mass 2 from some cyclic alkanes at 157 nm. The open circles are the experimental data points, while the solid curves are the fits to the spectra using the translational energy distributions of H_2 elimination as shown in Figure 13.

atoms of different sites. It is also important to point out that the C−C bond cleavage processes should be the dominant processes for the photodissociation of the branched alkanes, and the more branched alkanes produce more radical products from C−C bond fission, which subsequently crack into H^+ in the electron impact ionizer.

c. Photodissociation of Some Cyclic Alkanes. Photodissociation of cyclopropane, cyclopentane, cyclohexane, cycloheptane, and cyclooctane were also investigated in this work. TOF spectra of the photodissociation products from the cyclic alkanes at $m/e = 1$ (H) and 2 (H_2) were measured. All TOF spectra shown in this section were accumulated over 20−100-k laser shots.

TOF spectra at mass 1 from the cyclic alkanes are shown in Figure 10. Curve 2 and curve 3 of the TOF spectrum for cyclopropane come from the dissociative ionization of the momentum-matched CH_2 and C_2H_4 (CH_2 elimination) products, respectively. Curve 4 and curve 5 of the TOF spectrum for cyclopropane come from the dissociative ionization of the momentum-matched CH_3 and C_2H_3 (CH_3 elimination) products, respectively. TOF spectra at these high masses have also been measured. These products are attributed to the C−C bond fission processes. There are also small contributions of C−C bond fission processes for the higher cycloalkanes to the TOF spectra, but they are separated from the H-atom product channel and are not shown in Figure 10. Curve 1 for cyclopropane and all other curves in these TOF spectra should all be due to the H atom product channel for these molecules. These TOF spectra were simulated using the translational energy distributions presented in Figure 12. As one can see, there are three peaks in the distributions for cyclohexane, cycloheptane, and cyclooctane, which are peaked at ∼4, ∼13, and ∼28 kcal/mol, indicating that there are at least three different dynamical routes for the photodissociation of the larger cycloalkanes (cyclopentane to cyclooctane). The shape of the kinetic energy distribution of the H-atom elimination from cyclopropane (curve a) is clearly different from those of the rest of the cycloalkanes investigated. It seems that H-atom elimination from cyclopropane mainly produces slow H-atom products, which are probably due to secondary dissociation processes. It is important to note here

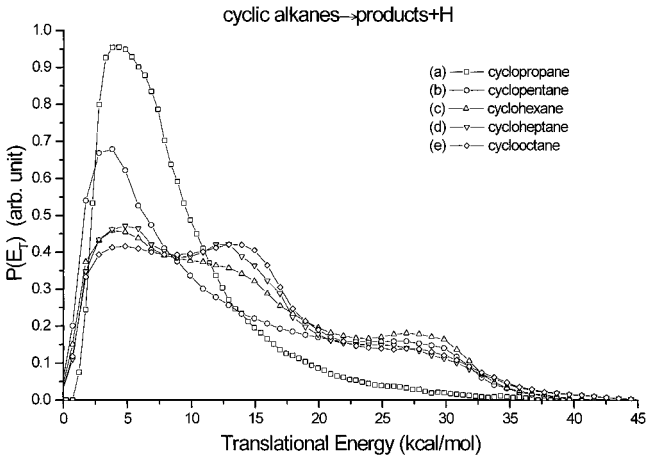

Figure 12. Translational energy distributions for atomic hydrogen (H) elimination from the photodissociation of some cyclic alkanes at 157 nm. The relative heights of the distributions are arbitrary.

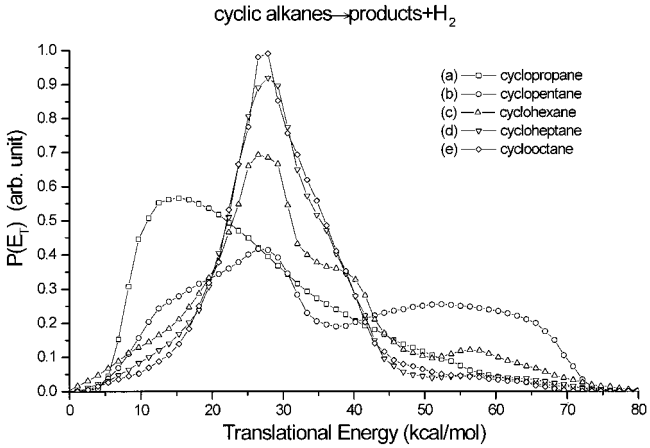

Figure 13. Translational energy distributions for molecular hydrogen (H_2) elimination from the photodissociation of some cyclic alkanes at 157 nm. The relative heights of the distributions are arbitrary.

that the CH_2 elimination to produce a methylene diradical and an ethylene molecule is the dominant process for the photodissociation of cyclopropane. In a comparison of Figure 12 with Figure 5, it is quite clear that the dynamics of H elimination from cyclic alkanes are notably different from those of the *n*-alkanes.

TOF spectra at $m/e = 2$ from the cyclic alkanes are shown in Figure 11. As pointed out above, all signals observed at $m/e = 2$ should come from the neutral H_2 photodissociation products. These TOF spectra were simulated using the translational energy distributions as shown in Figure 13. The translational energy distributions of the H_2 elimination for cyclohexane, cycloheptane, and cyclooctane are very similar to those for the *n*-alkanes (see Figure 6). The dominant H_2 elimination processes for these three molecules should be the three-center H_2 elimination processes (peaks at ~28 kcal/mol) from the CH_2 group, while the four-center H_2 elimination processes (peaks at ~57 kcal/mol) are minor. The kinetic energy distribution for the H_2 elimination products for cyclopropane and pentane are, however, significantly different from those of *n*-alkanes, indicating that the dynamics of H_2 elimination for these two molecules are quite different from other larger cyclic alkanes. This is likely due to the fact that electronic structures for small cyclic alkanes are significantly different from the larger ones because of the differences in ring strain between large and small cyclic alkanes. The fact that H_2 elimination from larger cyclic alkanes is similar to that of normal alkanes is interesting. This is likely due to the fact that the larger alkanes are similar in nature to the *n*-alkanes.

TABLE 3: Relative Yields of Atomic Hydrogen (H) and Molecular Hydrogen (H_2) Elimination Channels from the Photodissociation of Some Cyclic Alkanes

molecule	cycloalkanes → products+H	cycloalkanes → products+H_2
cyclopropane	1	0.16
cyclopentane	1	0.63
cyclohexane	1	1.3
cycloheptane	1	1.3
cyclooctane	1	1.6

The relative branching ratios for the H and H_2 elimination channels have also been determined and the results are listed in Table 3. The H elimination process is clearly more important for the photodissociation of cyclopropane and cyclopentane, while the H_2 elimination process is more important for the other higher cycloalkanes, which is similar to the *n*-alkanes. These results indicate that the dynamics of the photodissociation of cycloalkanes is related to the flexibility and the ring strain of the cycloalkanes.

IV. Conclusions

From the above experimental investigations, results of atomic and molecular hydrogen elimination from the photodissociation of alkanes at 157 nm are presented. Interesting dynamics of the atomic hydrogen (H) elimination and molecular hydrogen (H_2) elimination processes from the photodissociation of alkanes were observed. Generally speaking, the dynamics of the photodissociation of all different types of alkanes, acyclic and cyclic alkanes, are similar, while the relative yields of the different dissociation pathways are quite different. The competition of the H elimination, H_2 elimination, and the C−C bond rupture processes is mostly controlled by the complexities and the ring strain of the alkane species. It is also interesting to point out that even though the alkane molecules studied in this work are already quite large, the dissociation dynamics, however, are still quite nonstatistical in nature. More theoretical investigations are needed to understand the interesting dissociation dynamics of these alkane molecules.

Acknowledgment. This work was supported by the National Research Council, the Academia Sinica of the Republic of China, and the China Petroleum Corporation.

References and Notes

(1) Mordaunt, D. H.; Lambert, I. R.; Morley, G. P.; Ashfold, M. N. R.; Dixon, R. N.; Western, C. M.; Schnieder, L.; Welge, K. H. *J. Chem. Phys.* **1993**, *98*, 2054−2065.
(2) Heck, A. J. R.; Zare, R. N.; Chandler, D. W. *J. Chem. Phys.* **1996**, *104*, 3399−3402.
(3) Heck, A. J. R.; Zare, R. N.; Chandler, D. W. *J. Chem. Phys.* **1996**, *104*, 4019−4030.
(4) Wang, J.-H.; Liu, K. *J. Chem. Phys.* **1998**, *109*, 7105−7112.
(5) Brownsword, R. A.; Hillenkamp, M.; Laurent, T.; Vasta, R. K.; Volpp, H.-R.; Wolfrum, J. *Chem. Phys. Lett.* **1997**, *266*, 259−266.
(6) Mebel, A. M.; Lin, S. H.; Chang, C.-H.; *J. Chem. Phys.* **1997**, *106*, 2612−2620.
(7) Tonokura, K.; Matsumi, Y.; Kawasaki, M.; Kasatani, K. *J. Chem. Phys.* **1991**, *95*, 5065−5071.
(8) Jackson, W. M.; Price, R. J., II; Xu, D. D.; Wrobel, J. D.; Ahmed, M.; Peterka, D. S.; Suits, A. G. *J. Chem. Phys.* **1998**, *109*, 4703−4706.
(9) Okabe, H.; McNesby, J. R. *J. Chem. Phys.* **1961**, *34*, 668−669.
(10) Okabe, H.; McNesby, J. R. *J. Chem. Phys.* **1962**, 37, 1340−1346.
(11) Obi, K.; Akimoto, H.; Ogata, Y.; Tanaka, I. *J. Chem. Phys.* **1971**, *55*, 3822−3828.
(12) Okabe, H.; Becker, D. A. *J. Chem. Phys.* **1963**, *39*, 2549−2555.
(13) Sauer, M. C., Jr.; Dorfman, L. M. *J. Chem. Phys.* **1961**, *35*, 497−502.

(14) Mahan, B. H.; Mandal, R. *J. Chem. Phys*. **1962**, *37*, 207−211.
(15) Wu, S. M.; Lin, J. J.; Lee, Y. T.; Yang, X. *J. Chem. Phys*. **1999**, *111*, 1793−1796.
(16) Lin, J. J.; Harich, S.; Hwang, D. W.; Wu, S. M.; Lee, Y. T.; Yang, X. *J. Chin. Chem. Soc*. **1999**, *46*, 435−444.
(17) Lombos, B. A.; Sauvageau, P.; Sandorfy, C. *J. Mol. Spectrosc*. **1967**, *24*, 253−269.
(18) Lombos, B. A.; Sauvageau, P.; Sandorfy, C. *Chem. Phys. Lett*. **1967**, *1*, 42−43.
(19) Lombos, B. A.; Sauvageau, P.; Sandorfy, C. *Chem. Phys. Lett*. **1967**, *1*, 221−223.
(20) Lombos, B. A.; Sauvageau, P.; Sandorfy, C. *Chem. Phys. Lett*. **1967**, *1*, 382−384.
(21) Partridge, R. H. *J. Chem. Phys*. **1966**, *45*, 1685−1690.
(22) Katagiri, S.; Sandorfy, C. *Theor. Chim. Acta* **1966**, *4*, 203−223.
(23) Raymonda, J. W.; Simpson, W. T. *J. Chem. Phys*. **1967**, *47*, 430−448.
(24) Robin, M. B. *Higher Excited States of Polyatomic Molecules*; Academic Press: New York, 1974; Vol. 1, p 105, and references therein.
(25) Richartz, A.; Buenker, R. J.; Peyerimhoff, A. D. *Chem. Phys*. **1978**, *31*, 187−196.
(26) Galasso, V. *Chem. Phys*. **1992**, *161*, 189−197.
(27) Lin, J. J.; Hwang, D. W.; Harich, S.; Lee, Y. T.; Yang, X. *Rev. Sci. Instrum*. **1998**, *69*, 1642−1646.
(28) Harich, S. Ph.D. Thesis, University of California, Santa Barbara, 1999.
(29) Zhao, X. Ph.D. Thesis, University of California, Berkeley, 1988; Myers, J. D. Ph.D. Thesis, University of California, Berkeley, 1992.
(30) Tawara, H.; Kato, T. *Atom. Data Nucl. Data Tables* **1987**, *36*, 167.